ACS Macro Letters

Letter

Cite This: ACS Macro Lett. 2019, 8, 1617−1622

pubs.acs.org/macroletters

# Order-to-Disorder Transitions in Lamellar Melt Self-Assembled Core−Shell Bottlebrush Polymers

Michael G. Karavolias,[†] Jack B. Elder,[‡] Emily M. Ness,[§] and Mahesh K. Mahanthappa*[,†,‡]

[†]Department of Chemical Engineering and Materials Science, University of Minnesota, 421 Washington Avenue SE, Minneapolis, Minnesota 55455, United States

[‡]Department of Chemistry, University of Minnesota, 207 Pleasant Street SE, Minneapolis, Minnesota 55455, United States

[§]Department of Chemistry, Pacific Lutheran University, Rieke Science Center, 12180 Park Avenue S, Tacoma, Washington 98447, United States

Supporting Information

**ABSTRACT:** We report the synthesis and melt self-assembly behaviors of densely grafted, core−shell bottlebrush (csBB) polymers derived from covalently linking narrow dispersity, symmetric composition ABA-type triblock polymers through their chain midpoints. Derived from sequential ring-opening polymerizations of ε-decalactone and *rac*-lactide initiated from 5-norbornene-2-*exo*,3-*exo*-dimethanol, poly(lactide-*block*-ε-decalactone-*block*-lactide) macromonomers ($M_n$ = 9.2−17.8 kg/mol; $Đ$ = 1.19−1.25) were enchained by living ring-opening metathesis polymerization (ROMP) into csBBs with backbone degrees of polymerization $N_{bb}$ = 8−43. Temperature-dependent small-angle X-ray scattering (SAXS) studies indicate that the critical triblock arm degree of polymerization ($N_{arm}$) required for melt segregation decreases with increasing $N_{bb}$, leading to reductions in the accessible ordered lamellar microdomain ($d$) spacings. We derive a phenomenological relationship between the critical triblock arm segregation strength at the order−disorder transition $(\chi N_{arm})_{ODT}$ and $N_{bb}$ to enable the future design of microphase separated core−shell bottlebrushes, which self-assemble at sub-10 nm length scales for nanolithography and nanotemplating applications.

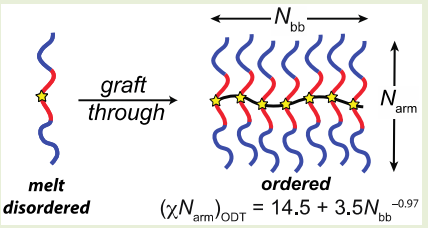


The self-assembly of segmented block polymers of chemically dissimilar monomers offers enticing opportunities to design nanostructured materials for value-added applications.[1−3] Narrow dispersity, linear AB diblock polymers self-assemble into ordered sphere packings, 3D networks, hexagonally-packed cylinders, and lamellae.[4] These segregated polymer melts balance the unfavorable enthalpy of A/B monomer contacts against configurational entropy losses associated with polymer chain stretching and polymer self−organization. The phase behaviors of AB diblocks depend on the volume composition of the A block $f_A = 1 - f_B$, the temperature-dependent effective A/B segmental interaction parameter ($\chi$), and the segment density-normalized degree of polymerization ($N$). Mean−field theories predict a volume fraction-dependent, minimum melt segregation strength at the order−disorder transition, $(\chi N)_{ODT}$, above which a diblock microphase separates.[5,6] Compositionally symmetric AB diblock polymers ($f_A = f_B = 0.5$) exhibit $(\chi N)_{ODT}$ = 10.5, and their lamellar microdomain periodicities scale as $d \sim \chi^{1/6} N^{2/3}$ in the strong segregation limit.[7] The magnitude of $\chi$, which depends on the chosen monomer chemistry, sets the minimum $N$ for melt segregation and, thus, the smallest accessible $d$-spacing. This thermodynamic lower bound curtails potential applications of block polymers as templates for advanced microelectronics[8,9] and mesoporous inorganic materials[10] with sub-10 nm features. Consequently, much attention has focused on discovering microphase-separated "high $\chi$/low $N$" diblock polymers toward ever smaller feature sizes for these applications.[8,11−22]

Manipulating molecular architecture offers a complementary yet nascent means of tuning A/B block polymer phase behavior[23,24] toward sub-10 nm templating, without resorting to new monomer chemistries. Mean-field theories predict that end-linking AB diblocks of length $N_{arm}$ into $(AB)_n$ star architectures reduces $(\chi N_{arm})_{ODT} \approx 5-6$ per arm, suggesting possible access to smaller $d$-spacings.[6,25] Early experiments on low $\chi$/high $N$ $(AB)_n$ stars reported only small reductions in $(\chi N)_{ODT}$,[26] with slight changes in the $d$-spacings[27] as compared to the parent AB diblocks. However, a more recent study by Sun et al. of lithium salt-doped, high $\chi$/low $N$ $(AB)_n$ stars ($n \leq 4$) established their ability to access domain spacings as small as $d$ = 9.7 nm.[28] This last report notably suggests that the critical $(\chi N_{arm})_{ODT}$ decreases with increasing arm number $n$ due to differences in translational entropy upon ordering into a periodic assembly. However, the synthesis of star block polymers with >4 arms becomes increasingly more difficult due to steric encumbrance arising from tethering the polymer chains to a single, small junction point.

Precision macromolecular syntheses of molecular bottlebrushes, in which polymer chains are end-linked through a

**Received:** October 5, 2019
**Accepted:** November 12, 2019
**Published:** November 25, 2019






DOI: 10.1021/acsmacrolett.9b00782
ACS Macro Lett. 2019, 8, 1617−1622

**Scheme 1. Synthesis of Core-Shell Bottlebrush Polymers (csBBs) from Poly(lactide-*block*-ε-decalactone-*block*-lactide) Macromonomers**

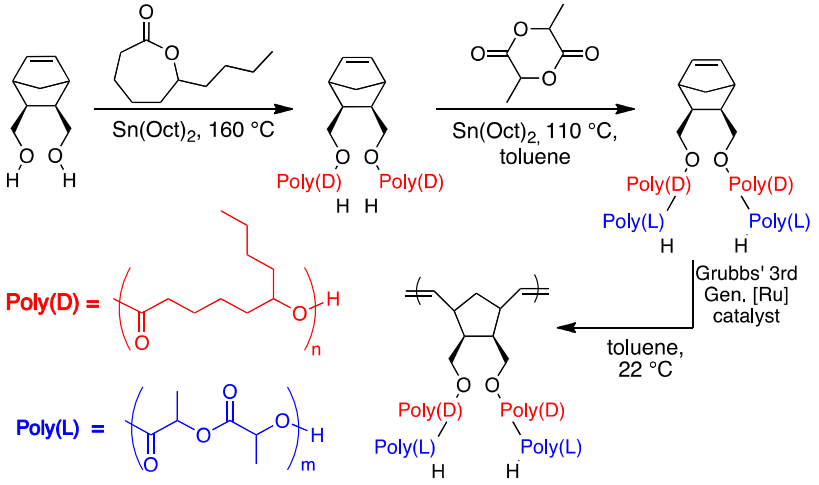


polymer backbone, have stimulated a plethora of studies of their melt self-assembly behaviors.[29,30] Numerous reports have examined the microphase separation of block polymers comprising bottlebrush A and bottlebrush B segments at large length scales $d$ = 50−200 nm, wherein the $d$-spacing depends primarily on the backbone degree of polymerization ($N_{bb}$).[31−36] On the other hand, Xia et al. established that randomly enchaining polymeric A and B arms into a random bottlebrush leads to microphase-separated lamellae, in which the $d$-spacing instead depends on the arm degrees of polymerization.[37] More recently, Johnson and co-workers showed that Janus-type graft block polymer bottlebrushes, in which the block junctions of AB diblocks are linked into a polymer backbone, form ordered morphologies with sub-10 nm microdomains by preorganizing melt-disordered AB diblock arms to self-assemble.[38,39] In spite of this useful result, access to these architectures is limited by complex, multifunctional inimer syntheses coupled with arduous preparative size-exclusion chromatography (SEC) purifications. On the other hand, the melt phase behaviors of well-known core−shell bottlebrushes (csBBs),[40−42] in which each backbone unit exhibits one or more AB diblock arms, remain poorly explored. Herein, we describe the syntheses and melt phase behaviors of densely grafted csBB polymers comprising high $\chi$/low $N$ ABA triblock arms linked through their chain midpoints.

We developed the modular "graft through"[30] synthesis of csBBs depicted in Scheme 1. 5-Norbornene-2-*exo*,3-*exo*-dimethanol (**1**), which derives from $LiAlH_4$ reduction of *cis*-5-norbornene-*exo*-2,3-dicarboxylic anhydride (see Supporting Information for synthetic details),[43] served as a difunctional initiator for bulk, Sn(oct)$_2$-catalyzed ring-opening transesterification polymerization (ROTEP) of ε-decalactone per the method of Martello et al.[44] Reaction aliquots of the resulting poly(ε-decalactone) (**D**) samples exhibited $M_{n,D}$ = 3.9−7.7 kg/mol by $^1$H NMR end group analyses (see Figure S1), with unimodal molar mass distributions and dispersities $Đ_D = M_w/M_n$ = 1.17−1.23 by SEC against poly(styrene) standards. One-pot, sequential chain extension polymerization of these macrodiols with *rac*-lactide yielded narrow dispersity poly(lactide-*block*-ε-decalactone-*block*-lactide) (**LDL**) triblocks with a norbornene functionality situated at the midblock center.[44] $^1$H NMR end group analyses reveal that these **LDL** triblocks exhibit $M_n$ = 9.2−17.8 kg/mol (see Figure S2) with nearly symmetric volume fractions $f_L$ = 0.51−0.52 (see Table S1 for detailed molecular characteristics), based on the homopolymer densities $\rho_D$ = 0.97 g/cm$^3$ and $\rho_L$ = 1.24 g/cm$^3$ at 22 °C.[44] SEC analyses against poly(styrene) standards establish the unimodality of the **LDL** triblock molar mass distributions with $Đ$ = 1.19−1.25.

**LDL** macromonomers were subjected to living ring-opening metathesis polymerization (ROMP) initiated by the bis-(pyridine) analog of Grubbs' third generation olefin metathesis catalyst (**G3**)[45] in toluene at 22 °C (Scheme 1). For each parent **LDL** triblock, we exploited the living characteristics of this polymerization to target csBBs with theoretical backbone degrees of polymerization $N_{bb,thy}$ = [**LDL**]/[**G3**] = 10, 20, 30, and 40. Polymerizations conducted with [**LDL**] = 15 mM typically proceeded to >97% macromonomer conversion to yield high purity **csLDL** bottlebrushes, thus, obviating the need for time-consuming purifications, as in the case of Janus-type bottlebrushes.[39] **csLDL** samples were characterized by SEC with multiangle laser light scattering (SEC-MALLS) detection in tetrahydrofuran (THF) at 25 °C (Figure 1) to measure directly their absolute molecular weights, $M_{n,csLDL}$. We calculated the observed backbone degrees of polymerization as $N_{bb,expt} = M_{n,csLDL}/M_{n,LDL}$ (Table 1).[46] Note that $M_{n,LDL}$ values were derived from $^1$H NMR end group analyses due to

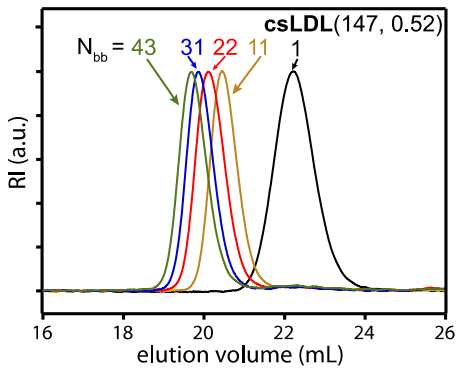


**Figure 1.** SEC trace overlay for the parent diblock **LDL**(147, 0.52) and daughter **csLDL**s with $N_{bb}$ = 11, 22, 31, and 43 from SEC-MALLS analysis, which were synthesized by targeting $N_{bb,thy}$ = 10, 20, 30, and 40.



DOI: 10.1021/acsmacrolett.9b00782
ACS Macro Lett. 2019, 8, 1617−1622

**Table 1. Molecular Characteristics of csLDL Block Polymer Bottlebrushes**

| csBB[a] | $M_{n,csLDL}$ (kg/mol) | $N_{bb,expt}$[b] | $Đ_{csLDL}$[b] | $T_{ODT}$[c] (°C) | $(\chi N_{arm})_{ODT}$ | $d$[d] (nm) |
|---|---|---|---|---|---|---|
| **LDL**(116, 0.52) | 9.2 | 1 | 1.20 | | | |
| **csLDL**(116, 0.52)−8 | 76.3 | 8 | 1.03 | 83 | 15.6 | 10.8 |
| **csLDL**(116, 0.52)−18 | 163 | 18 | 1.01 | 93 | 14.8 | 10.8 |
| **csLDL**(116, 0.52)−23 | 211 | 23 | 1.03 | 97 | 14.5 | 10.8 |
| **csLDL**(116, 0.52)−37 | 335 | 37 | 1.03 | 95 | 14.6 | 10.8 |
| **LDL**(147, 0.52) | 11.6 | 1 | 1.23 | 102 | 17.8 | 13.2 |
| **csLDL**(147, 0.52)−11 | 124 | 11 | 1.01 | 131 | 15.1 | 12.8 |
| **csLDL**(147, 0.52)−22 | 257 | 22 | 1.01 | 133 | 14.9 | 12.6 |
| **csLDL**(147, 0.52)−31 | 359 | 31 | 1.01 | 135 | 14.7 | 12.5 |
| **csLDL**(147, 0.52)−43 | 490 | 43 | 1.01 | 137 | 14.6 | 12.7 |
| **LDL**(178, 0.52) | 14.0 | 1 | 1.23 | 132 | 18.2 | 13.6 |
| **csLDL**(178, 0.52)−9 | 124 | 9 | 1.04 | 176 | 14.0 | 13.4 |
| **LDL**(186, 0.51) | 14.6 | 1 | 1.19 | 138 | 18.3 | 13.7 |
| **LDL**(227, 0.51) | 17.8 | 1 | 1.25 | 177 | 17.7 | 15.5 |

[a]Core−shell bottlebrushes identified as **csLDL**($N_{arm}f_L$)−$N_{bb,expt}$, where $N_{arm}$ is the segment density-normalized degree of polymerization of the **LDL** triblock macromonomer, $f_L$ is the poly(lactide) volume fraction, and $N_{bb,expt}$ is the experimentally determined backbone degree of polymerization. [b]$N_{bb,expt} = M_{n,csLDL}/M_{n,LDL}$, where $M_{n,csLDL}$ and $Đ_{csLDL}$ were determined by SEC-MALLS for $N_{bb,expt} > 1$, and $M_{n,LDL}$ was derived from $^1$H NMR end group analysis. [c]$T_{ODT}$ measured by temperature-dependent SAXS for all **csLDL** samples with $N_{bb,expt} > 1$. $T_{ODT}$ for **LDL** macromonomers was determined by DMS (see text for details). [d]Lamellar domain ($d$) spacing from SAXS at 28 °C.

the low $M_n$s of the **LDL** triblocks and their small refractive index increments ($dn/dc \leq 0.06$ mL/g), which prevented accurate SEC-MALLS measurements. The generally good agreement between $N_{bb,expt}$ in Table 1 and the targeted $N_{bb,thy}$ values is consistent with the living nature of the ROMP reaction. Thus, this synthetic strategy allows enchainment of narrow dispersity, symmetric triblocks with segment density-normalized degrees of polymerization $N_{arm}$ into a series of csBBs with defined backbone degrees of polymerization that are designated **csLDL**($N_{arm}f_L$)−$N_{bb,expt}$.

We examined the self-assembly behaviors of **LDL** triblock macromonomers and daughter **csLDL** bottlebrushes by synchrotron small-angle X-ray scattering (SAXS). Samples were solvent cast from toluene at 90−110 °C and subsequently annealed in vacuo at 130 °C for 2 h to remove residual solvent. Representative azimuthally integrated 1D-SAXS patterns for **csLDL**(116, 0.52) bottlebrushes are presented in Figure 2a. The broad, low intensity SAXS peak observed at 28 °C for macromonomer **LDL**(116, 0.52) and the absence of higher order scattering maxima are consistent with the correlation-hole scattering of a disordered block polymer melt.[47] However, homologous bottlebrushes with $N_{bb,expt}$ = 8, 18, 23, and 37 exhibit SAXS maxima at $(q/q^*)^2$ = 1, 4, and 9 ($q^*$ = 0.0588 Å$^{-1}$) consistent with their microphase separation into ordered lamellar phases. The expected extinction of the $(q/q^*)^2$ = 4 SAXS peak for a compositionally symmetric, lamellar block polymer is not observed as the volume fractions of these samples are slightly asymmetric with $f_L$ = 0.51−0.52. The observed ordered domain spacing $d$ = 10.8 nm is nearly invariant with increasing $N_{bb} \geq 10$. In sample series where the macromonomer is itself melt-segregated, we find that the $d$-spacings of the **csLDL** brushes are ∼1−3% smaller than those of the parent triblocks. Thus, we conclude that linking disordered **LDL** triblocks through their midpoints into csBB architectures drives their melt self-assembly, enabling ordering at smaller length scales than allowed by the linear triblock homologues. Johnson, Osuji, and co-workers observed a conceptually related architecture-driven ordering in Janus-type bottlebrush block polymers, in which disordered diblock polymer chains are linked through their block junctions.[39]

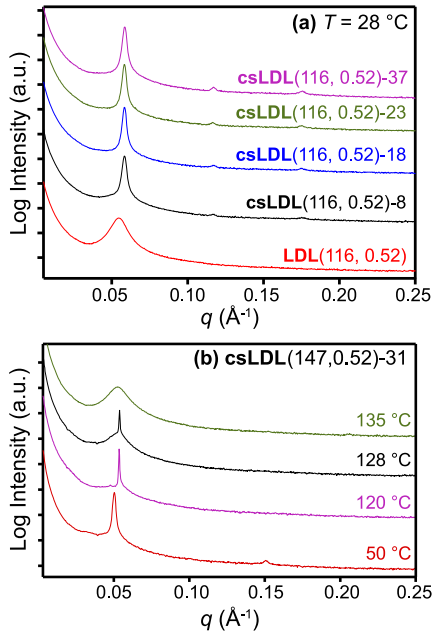


**Figure 2.** (a) 1D-SAXS intensity $I(q)$ vs scattering wavevector $q$ profiles for **LDL**(116, 0.52) and **csLDL** daughter samples at 28 °C, which demonstrate the melt-disordered **LDL** orders into a lamellar mesophase upon enchainment in a bottlebrush. (b) Temperature-dependent SAXS intensity profiles **csLDL**(147, 0.52)−31 establish that the sharp Bragg scattering associated with the lamellar morphology is replaced by broad, correlation-hole scattering of a disordered melt at $T_{ODT}$ = 135 °C.

We used temperature-dependent SAXS analyses to determine the order-to-disorder transition temperature ($T_{ODT}$) for each **csLDL** listed in Table 1. Figure 2b depicts representative 1D-SAXS intensity profiles for **csLDL**(147, 0.52)−31 between $T$ = 50−135 °C. We assign $T_{ODT}$ = 135 °C as the temperature at which all higher order scattering maxima and the sharp primary scattering peak at $q^*$ = 0.0537 Å$^{-1}$ are replaced by the weaker, broad correlation-hole scattering of a disordered block polymer melt.[47] $T_{ODT}$ values for **csLDL** ($N_{bb} > 1$) are reported in Table 1 for all samples that exhibit order-to-disorder



DOI: 10.1021/acsmacrolett.9b00782
ACS Macro Lett. 2019, 8, 1617−1622

transitions below the decomposition temperature (<180 °C). For the **LDL** macromonomers ($N_{bb}$ = 1), we used both SAXS and dynamic mechanical spectroscopy (DMS)[48,49] to determine $T_{ODT}$ (vide infra). The latter $T_{ODT}$ values agreed within 4 K (within 1%) between these two methods, and the values determined by DMS are presented in Table 1. From these data, we find that $T_{ODT}$ increases with increasing $N_{bb}$ for **csLDL**s derived from a given macromonomer.

In order to obtain quantitative insights into the self-assembly thermodynamics of csBB melts, we sought to calculate the critical $(\chi N_{arm})_{ODT}$ for each csBB reported in Table 1. By measuring the temperature-dependent, dynamic elastic storage shear modulus $G'(\omega)$ at a frequency $\omega$ = 1 rad/s and strain $|\gamma|$ = 1% in the linear viscoelastic regime, we identified $T_{ODT}$ for each **LDL** macromonomer as the temperature at which $G'(\omega)$ precipitously drops (see Figure S3).[48,49] We then calculated the value of $\chi_{LD}(T_{ODT})$ for each macromonomer from the mean-field theory result $(\chi N_{arm})_{ODT}$ = 17.996 for compositionally symmetric ABA-type triblock polymers.[6,50] The resulting values were fit to obtain the temperature-dependent effective interaction parameter $\chi_{LD}(T) = (97.0 \pm 25.8)/T - 0.138 \pm 0.063$ (see Figure S4). While the exact form of $\chi_{LD}(T)$ differs from that previously determined by Hillmyer and coworkers[44] using **LDL** triblocks synthesized analogously from benzene-1,4-dimethanol with $Đ \leq 1.18$ and $f_L$ = 0.46, values for $\chi_{LD}(T)$ calculated from both expressions agree within the stated error and they differ by <10% between $T$ = 80−180 °C. Discrepancies in $\chi_{LD}(T)$ may stem from differences in sample dispersity, composition, or chain midpoint functionality. Assuming that $\chi_{LD}(T)$ is independent of molecular architecture, we used the above expression to calculate $(\chi N_{arm})_{ODT}$ for the **LDL** triblock arms of each ordered csBB.

Figure 3 depicts a plot of $(\chi N_{arm})_{ODT}$ versus $N_{bb}$ for all **csLDL**$(N_{arm}, f_L)$ series, which demonstrates how the minimum

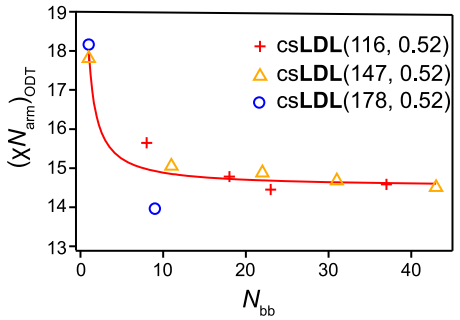


**Figure 3.** Plot of $(\chi N_{arm})_{ODT}$ vs $N_{bb}$ for **csLDL** bottlebrushes, which quantitatively demonstrates how the minimum arm segregation strength for csBB self-assembly decreases with backbone length. The solid red line represents an empirical data fit.

segregation strength $(\chi N_{arm})_{ODT}$ of the **LDL** triblock arms required for lamellar csBB ordering decreases with increasing $N_{bb}$. By fitting this curve, we obtained the phenomenological relationship (within a 95% confidence interval):

$$(\chi N_{arm})_{ODT} = (14.5 \pm 1.0) + (3.5 \pm 1.2) N_{bb}^{-0.97}$$

This expression suggests that as $N_{bb} \rightarrow \infty$, $(\chi N_{arm})_{ODT} \rightarrow$ 14.5. In other words, linking triblock polymers into a csBB architecture results in a 19% reduction in the minimum $N_{arm}$ required for microphase separation. Since the lamellar periodicity scales as $d \sim N^{\alpha}$ ($\alpha$ = 1/2 in weakly segregated melts, and $\alpha$ = 2/3 in strongly segregated systems),[5,51] polymerizing ABA triblocks through their midpoints into csBBs could facilitate access to $d$-spacings that are 10−13% smaller than those accessible from linear triblocks. In Figure 3, the most significant architecture-driven decrease in $(\chi N_{arm})_{ODT}$ is achieved when $1 \leq N_{bb} \leq 10$. The $T_{ODT}$ values in a given **csLDL**$(N_{arm} f_L)$ series become nearly invariant when $N_{bb}$ = 10−40. The fact that all of the data is captured by a single fit suggests the broad applicability of this expression for the design of melt self-assembled core−shell brush polymers. Note that this treatment assumes that the chemistry of the csBB backbone negligibly impacts the ordering behavior, given that the weight fraction of the backbone is small compared to that of the arms. In other words, this analysis assumes an athermal bottlebrush backbone.[33]

Spencer and Matsen recently reported self-consistent mean-field theory and field-theoretic simulations of graft polymers with AB diblock arms, in which they studied how backbone grafting density impacts their microphase separation.[52] These theoretical studies were stimulated by experiments of Maher et al.,[53] which demonstrated that graft polymers with symmetric AB diblock arms situated at 50% of the monomer units along a backbone exhibit $T_{ODT}$ values similar to those of the AB diblock arms. However, the results reported here differ significantly in that we observe increases in $T_{ODT}$, which presumably arise from the higher graft densities of the **csLDL** samples. Random phase approximation (RPA) predictions for csBBs with diblock arms appended to a backbone with grafting densities comparable to those considered here predict that the minimum $(\chi N_{diblock\ arm})_{ODT} \rightarrow$ ∼5−6 in the limit of large $N_{bb}$.[51] Since the RPA predicts that $(\chi N_{triblock})_{ODT}$ = 17.996 for a linear triblock and $(\chi N_{diblock})_{ODT}$ = 10.495 for linear diblock, we can recast the result $(\chi N_{triblock\ arm})_{ODT} \rightarrow$ 14.5 for the triblock arms of csBBs as $(\chi N_{diblock\ arm})_{ODT} \rightarrow 14.5(10.495/17.996) = 8.46$. Thus, our experimental observations trend in the direction of the RPA prediction, albeit with a slightly higher than expected asymptotic value in the limit $N_{bb} \rightarrow \infty$ likely due to fluctuation effects.

The thermodynamic stabilization of ordered lamellar morphologies of csBBs as compared to their linear ABA-type triblock analogs apparently stems from the covalent preorganization of triblocks for self-assembly depicted in Figure 4a. Cooling a disordered melt of linear ABA triblocks through $T_{ODT}$ drives enthalpically favorable demixing of dissimilar monomer segments, while incurring (1) an intrachain entropic penalty associated with chain stretching away from the interface, and (2) an ensemble entropy penalty due to A/B block junction localization at the microphase separated domain interfaces. On the other hand, covalently linking the midpoints of the ABA triblocks into a csBB architecture reduces the configurational entropy penalty for block junction ordering and to some small extent, the entropy loss on ABA chain stretching.[23] The csBBs exhibit $d$-spacings ∼1−3% smaller than those of the constituent triblock macromonomers. This situation differs from Janus-type brush block polymers, which derive from linking AB diblocks through their block junctions, wherein steric crowding near the backbone amplifies non-Gaussian chain stretching at the block junction to dilate the $d$-spacings by 8−10%.[38,39] We speculate that this csBB $d$-spacing contraction arises from frustrated space-filling at constant density in a lamellar morphology by cylindrically symmetric bottlebrushes, due to steric congestion at the backbone that


DOI: 10.1021/acsmacrolett.9b00782
ACS Macro Lett. 2019, 8, 1617−1622

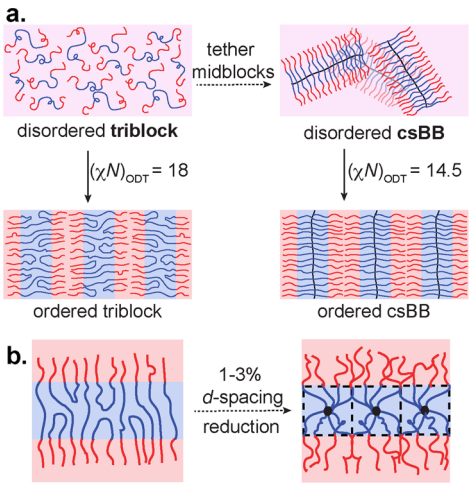


**Figure 4.** (a) Schematic depictions of the microphase separation of disordered linear ABA triblocks (left) and csBBs (right), which illustrate the reduced configurational entropy penalty for ordering due to covalent linking of the ABA triblock arms into a csBB. (b) Frustrated space-filling at constant density to maximize van der Waals cohesion in a lamellar morphology by a cylindrically symmetric csBB results in a slightly reduced lamellar *d*-spacing.

imposes restrictions on the arm conformations and on block junction placement (Figure 4b).

In summary, we have described a straightforward, three-step synthesis of csBB polymers and quantified their ability to melt microphase separate. Our studies reveal that covalently linking disordered, compositionally symmetric **LDL** triblock polymers into csBBs through a midchain functionality drives lamellar mesophase ordering, and enchaining ordered triblocks into csBBs increases their $T_{ODT}$s. By determining an expression for $\chi(T)$ for the monomer pair of interest and evaluating $(\chi N_{arm})_{ODT}$ for three distinct series of csBBs, we developed a quantitative relationship to describe how $(\chi N_{arm})_{ODT}$ decreases on increasing $N_{bb}$. This relationship, which may be universal for csBBs of different chemical compositions, will enable the design of block polymers that self-assemble at small length scales for future nanotemplating applications.

## ■ ASSOCIATED CONTENT

### Supporting Information

The Supporting Information is available free of charge at https://pubs.acs.org/doi/10.1021/acsmacrolett.9b00782.

Detailed synthetic procedures; representative $^1$H NMR spectra of poly(ε-decalactone) and poly(lactide-*block*-ε-decalactone-*block*-lactide); detailed molecular characterization data for **LDL** triblock macromonomers; DMS data for **LDL**(178, 0.52); fit of $\chi_{LD}(T)$ based on **LDL** macromonomer $T_{ODT}$ data (PDF)

## ■ AUTHOR INFORMATION

### Corresponding Author

*E-mail: maheshkm@umn.edu. Tel.: +1 (612) 625-4599.

### ORCID

Mahesh K. Mahanthappa: 0000-0002-9871-804X

### Notes

The authors declare no competing financial interest.

## ■ ACKNOWLEDGMENTS

This work was supported by National Science Foundation DMR-1708874, supplemented by a partial graduate fellowship from 3M Foundation (J.B.E.), and funding from the Research Experiences for Undergraduates (REU) Program of the National Science Foundation under Award Number DMR-1559833 and through the University of Minnesota MRSEC under Award Number DMR-1420013 (E.M.N.). Preliminary SAXS analyses were acquired in the Characterization Facility at the University of Minnesota, which also receives partial support from NSF through the UMN MRSEC (DMR-1420013). Synchrotron SAXS experiments were conducted at the 12-ID-B beamline of the Advanced Photon Source, a U.S. Department of Energy (DOE) Office of Science User Facility operated by Argonne National Laboratory under Contract No. DE-AC02-06CH11357.

## ■ REFERENCES

(1) Bates, C. M.; Bates, F. S. 50th Anniversary Perspective: Block Polymers—Pure Potential. *Macromolecules* **2017**, *50*, 3−22.
(2) Bates, F. S.; Hillmyer, M. A.; Lodge, T. P.; Bates, C. M.; Delaney, K. T.; Fredrickson, G. H. Multiblock Polymers: Panacea or Pandora's Box? *Science* **2012**, *336*, 434−440.
(3) Ruzette, A.-V.; Leibler, L. Block Copolymers in Tomorrow's Plastics. *Nat. Mater.* **2005**, *4*, 19−31.
(4) Abetz, V.; Simon, P. F. W. Phase Behaviour and Morphologies of Block Copolymers. In *Block Copolymers I*; Abetz, V., Ed.; Springer: Berlin, Heidelberg, 2005; pp 125−212.
(5) Leibler, L. Theory of Microphase Separation in Block Copolymers. *Macromolecules* **1980**, *13*, 1602−1617.
(6) Matsen, M. W. Effect of Architecture on the Phase Behavior of AB-Type Block Copolymer Melts. *Macromolecules* **2012**, *45*, 2161−2165.
(7) Bates, F. S.; Fredrickson, G. H. Block Copolymers: Designer Soft Materials. *Phys. Today* **1999**, *52*, 32−38.
(8) Sinturel, C.; Bates, F. S.; Hillmyer, M. A. High χ−Low *N* Block Polymers: How Far Can We Go? *ACS Macro Lett.* **2015**, *4*, 1044−1050.
(9) Bates, C. M.; Maher, M. J.; Janes, D. W.; Ellison, C. J.; Willson, C. G. Block Copolymer Lithography. *Macromolecules* **2014**, *47*, 2−12.
(10) Orilall, M. C.; Wiesner, U. Block Copolymer Based Composition and Morphology Control in Nanostructured Hybrid Materials for Energy Conversion and Storage: Solar Cells, Batteries, and Fuel Cells. *Chem. Soc. Rev.* **2011**, *40*, 520−535.
(11) Son, J. G.; Chang, J.-B.; Berggren, K. K.; Ross, C. A. Assembly of Sub-10-nm Block Copolymer Patterns with Mixed Morphology and Period Using Electron Irradiation and Solvent Annealing. *Nano Lett.* **2011**, *11*, 5079−5084.
(12) Durand, W. J.; Blachut, G.; Maher, M. J.; Sirard, S.; Tein, S.; Carlson, M. C.; Asano, Y.; Zhou, S. X.; Lane, A. P.; Bates, C. M.; Ellison, C. J.; Willson, C. G. Design of High-χ Block Copolymers for Lithography. *J. Polym. Sci., Part A: Polym. Chem.* **2015**, *53*, 344−352.
(13) Cushen, J. D.; Otsuka, I.; Bates, C. M.; Halila, S.; Fort, S.; Rochas, C.; Easley, J. A.; Rausch, E. L.; Thio, A.; Borsali, R.; Willson, C. G.; Ellison, C. J. Oligosaccharide/Silicon-Containing Block Copolymers with 5 nm Features for Lithographic Applications. *ACS Nano* **2012**, *6*, 3424−3433.
(14) Ober, C. K. A Dress Code for Block Copolymers. *Nat. Nanotechnol.* **2017**, *12*, 507.
(15) Yu, D. M.; Smith, D. M.; Kim, H.; Rzayev, J.; Russell, T. P. Two-Step Chemical Transformation of Polystyrene-Block-Poly(solketal acrylate) Copolymers for Increasing χ. *Macromolecules* **2019**, *52*, 6458−6466.
(16) Yoshida, K.; Tian, L.; Miyagi, K.; Yamazaki, A.; Mamiya, H.; Yamamoto, T.; Tajima, K.; Isono, T.; Satoh, T. Facile and Efficient Modification of Polystyrene-*block*-Poly(methyl methacrylate) for



DOI: 10.1021/acsmacrolett.9b00782
*ACS Macro Lett.* 2019, 8, 1617−1622

Achieving Sub-10 nm Feature Size. *Macromolecules* **2018**, *51*, 8064−8072.
(17) Azuma, K.; Sun, J.; Choo, Y.; Rokhlenko, Y.; Dwyer, J. H.; Schweitzer, B.; Hayakawa, T.; Osuji, C. O.; Gopalan, P. Self-Assembly of an Ultrahigh-$\chi$ Block Copolymer with Versatile Etch Selectivity. *Macromolecules* **2018**, *51*, 6460−6467.
(18) Chen, Q. P.; Barreda, L.; Oquendo, L. E.; Hillmyer, M. A.; Lodge, T. P.; Siepmann, J. I. Computational Design of High-$\chi$ Block Oligomers for Accessing 1 nm Domains. *ACS Nano* **2018**, *12*, 4351−4361.
(19) Kwak, J.; Mishra, A. K.; Lee, J.; Lee, K. S.; Choi, C.; Maiti, S.; Kim, M.; Kim, J. K. Fabrication of Sub-3 nm Feature Size Based on Block Copolymer Self-Assembly for Next-Generation Nanolithography. *Macromolecules* **2017**, *50*, 6813−6818.
(20) Carter, M. C. D.; Jennings, J.; Speetjens, F. W.; Lynn, D. M.; Mahanthappa, M. K. A Reactive Platform Approach for the Rapid Synthesis and Discovery of High $\chi$/Low $N$ Block Polymers. *Macromolecules* **2016**, *49*, 6268−6276.
(21) Oschmann, B.; Lawrence, J.; Schulze, M. W.; Ren, J. M.; Anastasaki, A.; Luo, Y.; Nothling, M. D.; Pester, C. W.; Delaney, K. T.; Connal, L. A.; McGrath, A. J.; Clark, P. G.; Bates, C. M.; Hawker, C. J. Effects of Tailored Dispersity on the Self-Assembly of Dimethylsiloxane−Methyl Methacrylate Block Co-Oligomers. *ACS Macro Lett.* **2017**, *6*, 668−673.
(22) Sweat, D. P.; Kim, M.; Larson, S. R.; Choi, J. W.; Choo, Y.; Osuji, C. O.; Gopalan, P. Rational Design of a Block Copolymer with a High Interaction Parameter. *Macromolecules* **2014**, *47*, 6687−6696.
(23) Park, J.; Jang, S.; Kon Kim, J. Morphology and Microphase Separation of Star Copolymers. *J. Polym. Sci., Part B: Polym. Phys.* **2015**, *53*, 1−21.
(24) Buzza, D. M. A.; Hamley, I. W.; Fzea, A. H.; Moniruzzaman, M.; Allgaier, J. B.; Young, R. N.; Olmsted, P. D.; McLeish, T. C. B. Anomalous Difference in the Order−Disorder Transition Temperature Comparing a Symmetric Diblock Copolymer AB with Its Hetero-Four-Arm Star Analog $A_2B_2$. *Macromolecules* **1999**, *32*, 7483−7495.
(25) Olvera de la Cruz, M.; Sanchez, I. C. Theory of Microphase Separation in Graft and Star Copolymers. *Macromolecules* **1986**, *19*, 2501−2508.
(26) Floudas, G.; Pispas, S.; Hadjichristidis, N.; Pakula, T.; Erukhimovich, I. Microphase Separation in Star Block Copolymers of Styrene and Isoprene. Theory, Experiment, and Simulation. *Macromolecules* **1996**, *29*, 4142−4154.
(27) Ishizu, K.; Uchida, S. Synthesis and Microphase-Separated Structures of Star-Block Copolymers. *Prog. Polym. Sci.* **1999**, *24*, 1439−1480.
(28) Sun, Z.; Zhang, W.; Hong, S.; Chen, Z.; Liu, X.; Xiao, S.; Coughlin, E. B.; Russell, T. P. Using Block Copolymer Architecture to Achieve Sub-10 nm Periods. *Polymer* **2017**, *121*, 297−303.
(29) Rzayev, J. Molecular Bottlebrushes: New Opportunities in Nanomaterials Fabrication. *ACS Macro Lett.* **2012**, *1*, 1146−1149.
(30) Verduzco, R.; Li, X.; Pesek, S. L.; Stein, G. E. Structure, Function, Self-Assembly, and Applications of Bottlebrush Copolymers. *Chem. Soc. Rev.* **2015**, *44*, 2405−2420.
(31) Runge, M. B.; Dutta, S.; Bowden, N. B. Synthesis of Comb Block Copolymers by ROMP, ATRP, and ROP and Their Assembly in the Solid State. *Macromolecules* **2006**, *39*, 498−508.
(32) Rzayev, J. Synthesis of Polystyrene−Polylactide Bottlebrush Block Copolymers and Their Melt Self-Assembly into Large Domain Nanostructures. *Macromolecules* **2009**, *42*, 2135−2141.
(33) Dalsin, S. J.; Rions-Maehren, T. G.; Beam, M. D.; Bates, F. S.; Hillmyer, M. A.; Matsen, M. W. Bottlebrush Block Polymers: Quantitative Theory and Experiments. *ACS Nano* **2015**, *9*, 12233−12245.
(34) Gai, Y.; Song, D.-P.; Yavitt, B. M.; Watkins, J. J. Polystyrene-*block*-Poly(ethylene oxide) Bottlebrush Block Copolymer Morphology Transitions: Influence of Side Chain Length and Volume Fraction. *Macromolecules* **2017**, *50*, 1503−1511.
(35) Lin, T.-P.; Chang, A. B.; Luo, S.-X.; Chen, H.-Y.; Lee, B.; Grubbs, R. H. Effects of Grafting Density on Block Polymer Self-Assembly: From Linear to Bottlebrush. *ACS Nano* **2017**, *11*, 11632−11641.
(36) Liberman-Martin, A. L.; Chu, C. K.; Grubbs, R. H. Application of Bottlebrush Block Copolymers as Photonic Crystals. *Macromol. Rapid Commun.* **2017**, *38*, 1700058.
(37) Xia, Y.; Olsen, B. D.; Kornfield, J. A.; Grubbs, R. H. Efficient Synthesis of Narrowly Dispersed Brush Copolymers and Study of Their Assemblies: The Importance of Side Chain Arrangement. *J. Am. Chem. Soc.* **2009**, *131*, 18525−18532.
(38) Kawamoto, K.; Zhong, M.; Gadelrab, K. R.; Cheng, L.-C.; Ross, C. A.; Alexander-Katz, A.; Johnson, J. A. Graft-through Synthesis and Assembly of Janus Bottlebrush Polymers from A-*branch*-B Diblock Macromonomers. *J. Am. Chem. Soc.* **2016**, *138*, 11501−11504.
(39) Guo, Z.-H.; Le, A. N.; Feng, X.; Choo, Y.; Liu, B.; Wang, D.; Wan, Z.; Gu, Y.; Zhao, J.; Li, V.; Osuji, C. O.; Johnson, J. A.; Zhong, M. Janus Graft Block Copolymers: Design of a Polymer Architecture for Independently Tuned Nanostructures and Polymer Properties. *Angew. Chem., Int. Ed.* **2018**, *57*, 8493−8497.
(40) Zhang, M.; Müller, A. H. E. Cylindrical Polymer Brushes. *J. Polym. Sci., Part A: Polym. Chem.* **2005**, *43*, 3461−3481.
(41) Lee, H.-i.; Jakubowski, W.; Matyjaszewski, K.; Yu, S.; Sheiko, S. S. Cylindrical Core−Shell Brushes Prepared by a Combination of ROP and ATRP. *Macromolecules* **2006**, *39*, 4983−4989.
(42) Huang, K.; Rzayev, J. Well-Defined Organic Nanotubes from Multicomponent Bottlebrush Copolymers. *J. Am. Chem. Soc.* **2009**, *131*, 6880−6885.
(43) Long, T. R.; Maity, P. K.; Samarakoon, T. B.; Hanson, P. R. ROMP-Derived Oligomeric Phosphates for Application in Facile Benzylation. *Org. Lett.* **2010**, *12*, 2904−2907.
(44) Martello, M. T.; Schneiderman, D. K.; Hillmyer, M. A. Synthesis and Melt Processing of Sustainable Poly($\epsilon$-decalactone)-*block*-Poly(lactide) Multiblock Thermoplastic Elastomers. *ACS Sustainable Chem. Eng.* **2014**, *2*, 2519−2526.
(45) Bates, C. M.; Chang, A. B.; Momčilović, N.; Jones, S. C.; Grubbs, R. H. ABA Triblock Brush Polymers: Synthesis, Self-Assembly, Conductivity, and Rheological Properties. *Macromolecules* **2015**, *48*, 4967−4973.
(46) Pesek, S. L.; Li, X.; Hammouda, B.; Hong, K.; Verduzco, R. Small-Angle Neutron Scattering Analysis of Bottlebrush Polymers Prepared Via Grafting-through Polymerization. *Macromolecules* **2013**, *46*, 6998−7005.
(47) Bates, F. S. Measurement of the Correlation Hole in Homogeneous Block Copolymer Melts. *Macromolecules* **1985**, *18*, 525−528.
(48) Rosedale, J. H.; Bates, F. S. Rheology of Ordered and Disordered Symmetric Poly(ethylenepropylene)-Poly(ethylethylene) Diblock Copolymers. *Macromolecules* **1990**, *23*, 2329−2338.
(49) Cochran, E. W.; Bates, F. S. Thermodynamic Behavior of Poly(cyclohexylethylene) in Polyolefin Diblock Copolymers. *Macromolecules* **2002**, *35*, 7368−7374.
(50) Wu, L.; Cochran, E. W.; Lodge, T. P.; Bates, F. S. Consequences of Block Number on the Order−Disorder Transition and Viscoelastic Properties of Linear $(AB)_n$ Multiblock Copolymers. *Macromolecules* **2004**, *37*, 3360−3368.
(51) Fredrickson, G. H.; Helfand, E. Fluctuation Effects in the Theory of Microphase Separation in Block Copolymers. *J. Chem. Phys.* **1987**, *87*, 697−705.
(52) Spencer, R. K. W.; Matsen, M. W. Field-Theoretic Simulations of Bottlebrush Copolymers. *J. Chem. Phys.* **2018**, *149*, 184901.
(53) Maher, M. J.; Jones, S. D.; Zografos, A.; Xu, J.; Schibur, H. J.; Bates, F. S. The Order−Disorder Transition in Graft Block Copolymers. *Macromolecules* **2018**, *51*, 232−241.



DOI: 10.1021/acsmacrolett.9b00782
*ACS Macro Lett.* 2019, 8, 1617−1622